Monte Carlo study of magnetic structures in rare-earth amorphous alloys

Alexey Bondarev* and *Igor* Bataronov

Voronezh State Technical University, 14 Moskovski prospekt, 394026 Voronezh, Russian Federation

Abstract. Using the Monte Carlo method, we studied magnetic properties of the models of Re-Tb and Re-Gd amorphous alloys as well as pure amorphous Tb and Gd. The magnetic phase diagrams for the models of amorphous Tb and Gd were constructed. We determined the values of D/J_0 (for Tb) and $J_1/|J_2|$ (for Gd) at which the transition into spin-glass-like state takes place. The local magnetic structure was studied by the spin correlation functions and the angular spin correlation functions. The difference in magnetic structures in amorphous alloys with the random anisotropy and with fluctuations of exchange interaction was revealed.

1 Introduction

Spin glasses are of great interest as a new class of magnetic materials having the unique physical properties [1, 2].

Binary amorphous alloys of heavy rare-earth metals (REM) with nonmagnetic transition metals are very little studied, although in this case the transition to the spin-glass state takes place. In amorphous alloys of the rhenium-terbium (Re-Tb) and rhenium-gadolinium (Re-Gd) systems the typical for spin glasses maximum on the temperature dependence of dynamic magnetic susceptibility $\chi(T)$ and irreversibility of magnetization *M(T)* were experimentally revealed [3].

However, the nature of the spin-glass state on the microscopic level is studied insufficiently. This encourages us to construct and analyze computer models of atomic structure and magnetic properties of these materials.

As an object of our study, we chose the Re-Tb system with the strong random anisotropy and the Re-Gd system with fluctuations of exchange interactions. The choice of these alloys is caused by the prospects of their application as memory elements.

2 Simulation Technique

Using the molecular dynamics method, we constructed the models of atomic structure of the Re-Tb and Re-Gd amorphous alloys and of pure amorphous Tb and Gd in the wide compositional region. Each model consisted of 100 000 atoms. Interatomic interaction was described by an empirical polynomial potential [4]. The radial distribution functions (RDFs) calculated for the models are in good agreement with the results of the X-ray diffraction experiment [5].

Using the Monte Carlo method in the frame of the Heisenberg model, we carried out simulation of magnetic properties of Re-Tb amorphous alloys and of pure amorphous Tb. The standard Metropolis algorithm of the Monte Carlo method was used [6]. Exchange interaction between the neighbouring magnetic ions as well as the random magnetic anisotropy play the most important role in forming of the magnetically ordered structures in amorphous alloys containing REM. Therefore, we used the following model Hamiltonian [7]:

$$H = -\frac{1}{2}\sum_{i,j} J_{ij}\left(\vec{S}_i \cdot \vec{S}_j\right) - D\sum_i \left(\vec{n}_i \cdot \vec{S}_i\right)^2, \quad (1)$$

where J_{ij} is exchange integral between the spins *i* and *j*; D is anisotropy constant; S_i is classical Heisenberg spin; n_i is unit vector determining the direction of the local anisotropy axes.

Dependence of the exchange integral on the interatomic distance *r* was chosen as a linear function:

$$J(r) = \begin{cases} J_0 \dfrac{r_{\min} - r}{r_{\min} - r_1}, & r \le r_{\min} \\ 0, & r > r_{\min} \end{cases}, \quad (2)$$

where $J_0 = 19,26\,\mathrm{K}$ is average value of the exchange integral which is equal to the corresponding value for crystalline Tb; r_1 is position of the first peak on the partial pair RDF $g_{Tb\text{-}Tb}(r)$; r_{min} is position of the first minimum of the $g_{Tb\text{-}Tb}(r)$ function.

Directions of local anisotropy axes were chosen randomly at each site. The value of anisotropy constant in this model varied in a wide region ($D/J_0 = 0-20$).

* Corresponding author: bondarev_a_v@mail.ru

We chose the random anisotropy constant for the Re-Tb alloys linearly dependent on the concentration of Tb atoms:

$$D/J_0 = 6,6 \cdot x/100, \quad (3)$$

where x is concentration of Tb atoms, %. For pure terbium (x = 100 at. %) this formula yields $D/J_0 = 6,6$.

For amorphous Gd and Re-Gd amorphous alloys the Hamiltonian was chosen as follows [8]:

$$H = -\frac{1}{2}\sum_{i,j} J_1\left(\vec{S}_i \cdot \vec{S}_j\right) - \frac{1}{2}\sum_{i,k} J_2\left(\vec{S}_i \cdot \vec{S}_k\right), \quad (4)$$

where $J_1 > 0$ is exchange integral among spins which are in the distances not exceeding $r_1^{\min} = 0,455$ nm – the position of the first minimum of the pair RDF $g(r)$; $J_2 < 0$ is exchange integral among spins which are in the distances in the interval from $r_1^{\min}$ to $r_2^{\min} = 0,770$ nm – the first and second minima of the pair RDF $g(r)$.

The value of the exchange integral in the second coordination sphere J_2 varied in a wide range ($J_1/|J_2| = 2-16$).

3 Magnetic phase diagram for amorphous Tb

For the model of pure amorphous Tb we calculated the temperature dependencies of spontaneous magnetization (Fig. 1) at different values of ratio of the anisotropy constant to the average value of the exchange integral D/J_0. Analyzing the *M(T)* curves, we can conclude that at $D/J_0 = 0$ in the system the ferromagnetic ordering takes place ($M/M_S = 1$ where M_S is saturation magnetization), at $D/J_0 > 0$ – the asperomagnetic ordering ($M/M_S < 1$) which is typical for spin glasses with high concentrations of the REM atoms.

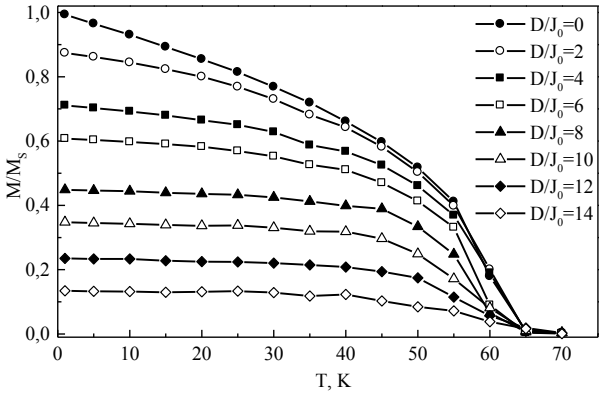

Fig. 1. Temperature dependence of spontaneous magnetization with different D/J_0 values for the model of amorphous Tb

The temperatures of magnetic phase transitions were determined as the positions of peaks on the temperature dependencies of magnetic susceptibility $\chi(T)$. The values of susceptibility were obtained during cooling of the model, and at each temperature the values were averaged over 10 cycles of 10^3 MC-steps/spin.

As a result, we obtained the magnetic phase diagram for amorphous Tb in the $D/J_0 - T$ coordinates (Fig. 2). It allows one to determine the phase state of the system depending on the emperature and the value of anisotropy constant.

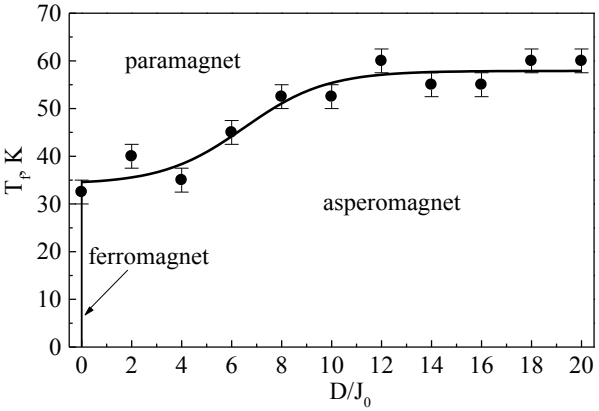

Fig. 2. Magnetic phase diagram $T_f(D/J_0)$ for the model of amorphous Tb

4 Magnetic phase diagram for Re-Tb amorphous alloys

We also studied magnetic properties of the models of $Re_{100-x}Tb_x$ (x = 5, 10, 13, 15, 20, 29, 49, 59 and 91 at. %) amorphous alloys.

In all the models the transition to the spin-glass-like state was observed (Fig. 3), except of $Re_{95}Tb_5$ and $Re_{90}Tb_{10}$ where the paramagnetic phase exists in the entire temperature region up to 1 K. Magnetization at low temperatures for all compositions did not exceed $0,1M_S$. With increasing concentration of Tb atoms the transition temperature linearly increases. This linear dependence qualitatively agrees with the experimental results [3].

The spin-glass transition takes place only if the concentration of Tb atoms $x \geq 13$ at. %, i.e. above the percolation threshold in this system.

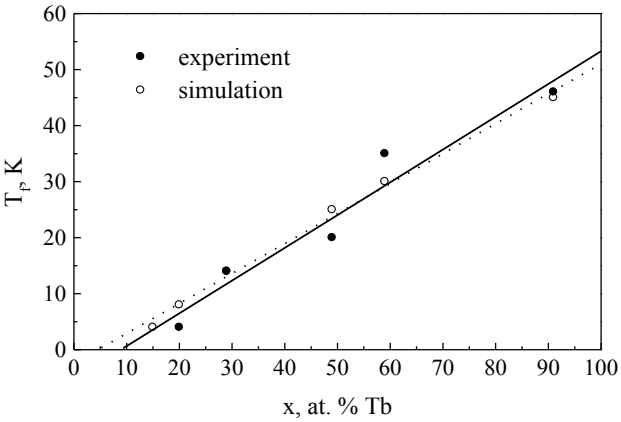

Fig. 3. Compositional dependence of the spin-glass transition temperature for the models of Re-Tb amorphous alloys

5 Spin correlation functions of amorphous Tb

For the models of pure amorphous Tb, the spin correlation functions were calculated (Fig. 4):

$$K(r) = \left\langle \vec{S}(r) \cdot \vec{S}(0) \right\rangle . \quad (5)$$

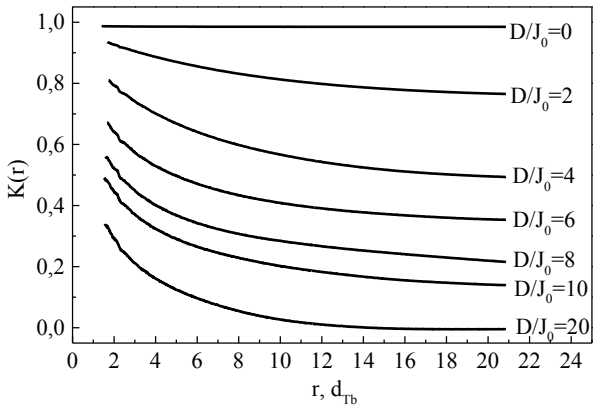

Fig. 4. Spin correlation functions for the model of amorphous Tb (T = 1 K) at various values of the D/J_0 ratio

At all the values of D/J_0, the $K(r)$ functions exponentially decrease with distance:

$$K(r) = K_0 + Ae^{-\frac{r-r_0}{\xi}}, \quad (6)$$

where K_0, A, r_0 are constants; ξ is correlation length.

We calculated the dependence of the correlation length ξ from the approximation of the $K(r)$ function by the eq. (6) on D/J_0 for amorphous Tb at T = 1 K (Fig. 5). In Fig. 5 d_{Tb} is the diameter of the terbium atom (d_{Tb} = 0.354 nm).

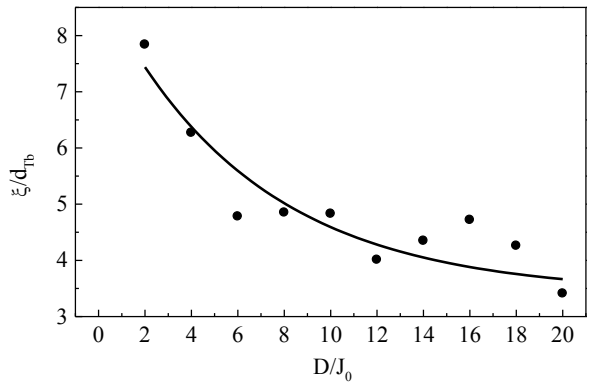

Fig. 5. Dependence of the correlation length on the D/J_0 value for the model of amorphous Tb (T = 1 K)

The temperature dependence of the correlation length for the model of amorphous Tb at $D/J_0 = 6,6$ is shown in Fig. 6. Near the phase transition temperature T_f the correlation length sharply decreases, and in the paramagnetic phase it is near one diameter of Tb atom.

For these models we also calculated the angular spin correlation functions $P(\theta)$ which are the distribution functions of the angles between directions of spins arranged within the first coordination sphere (Fig. 7). The $P(\theta)$ functions characterize the local magnetic ordering in this system. All these functions have one distinct maximum, its position θ_{max} monotonically increase with increasing the D/J_0 value.

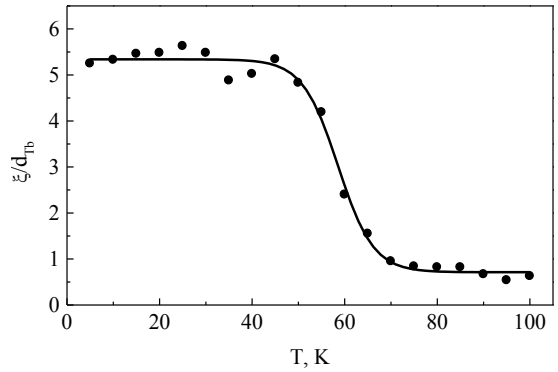

Fig. 6. Temperature dependence of the correlation length for the model of amorphous Tb at $D/J_0 = 6,6$

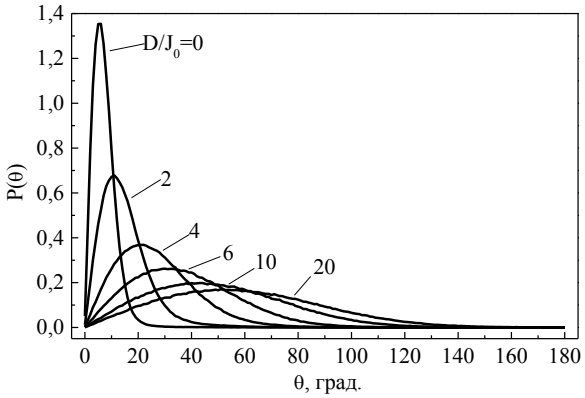

Fig. 7. Angular spin correlation functions for the model of amorphous Tb at $T = 1$ K

6 Magnetic phase diagram for amorphous Gd

For the model of pure amorphous Gd, we calculated the temperature dependencies of spontaneous magnetization M at variuos values of the $J_1/|J_2|$ ratio ($J_1/|J_2| = 10$, 11, 12, 13 и 14). In the Fig. 8 we present the dependence maximum spontaneous magnetization (at T = 1 K) on the $J_1/|J_2|$ ratio for the model of amorphous Gd.

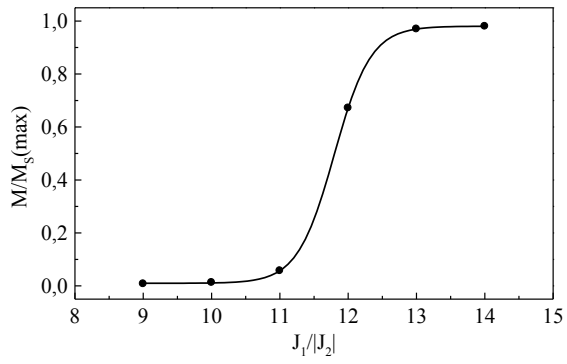

Fig. 8. Dependence of maximum spontaneous magnetization (at T = 1 K) on the $J_1/|J_2|$ ratio for the model of amorphous Gd

At the low temperatures at $J_1/|J_2| \geq 13$ the ferromagnetic state takes place, at $11 < J_1/|J_2| < 13$ – the asperomagnetic state, and at $J_1/|J_2| \leq 11$ the system transits into the spin-glass state.

Thus, we obtained the magnetic phase diagram for amorphous Gd in the $J_1/|J_2|$ – T coordinates (Fig. 9). It allows one to determine the phase state of the system depending on the temperature and the exchange integral within the second coordination sphere J_2.

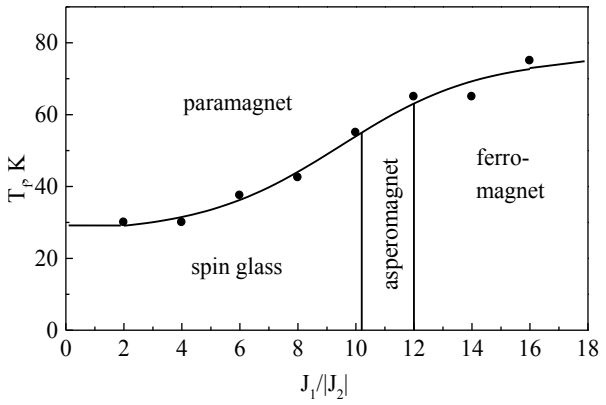

Fig. 9. Magnetic phase diagram $T_f\left(J_1/|J_2|\right)$ for the model of amorphous Gd

For the models of Re-Gd amorphous alloys with $J_1/|J_2| = 10$ the transition into spin-glass state is observed. The temperature dependence of the transition temperature is linear and agrees well with the experimental results [3].

7 Spin correlation functions of amorphous Gd

In Fig. 10 we present the spin correlation functions $K(r)$ for the model of amorphous Gd calculated at the values $J_1/|J_2| = 9$, 10, 11, 12, 13 and the temperature $T = 1$ K. The values $J_1/|J_2| = 9$, 10, 11 correspond to the spin-glass state, $J_1/|J_2| = 12$ – asperomagnet, and $J_1/|J_2| = 13$ – ferromagnetic state. In the spin-glass phase, the $K(r)$ functions oscillate in the large distances. This indicates of positive as well as negative correlations in arrangement of magnetic moments of the Gd atoms.

The difference between spin correlation functions with the random anisotropy and with fluctuations of exchange interaction for Tb-based and Gd-based amorphous alloys indicates of the difference in magnetic structures in amorphous alloys with the random anisotropy and with fluctuations of exchange interaction.

In Fig. 11 we present the angular spin correlation functions $P(\theta)$ for the model of amorphous Gd calculated at $J_1/|J_2| = 6$, 8, 10, 12 and the temperature $T = 1$ K.

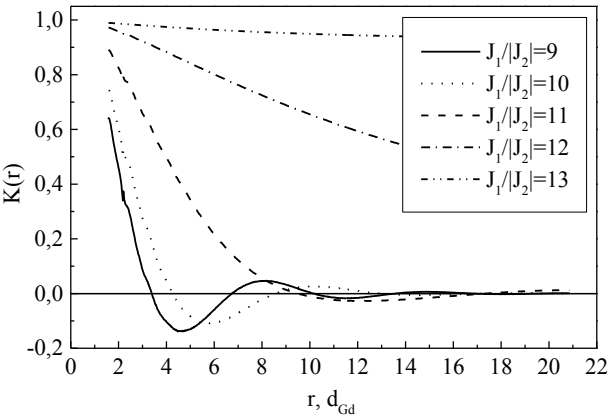

Fig. 10. Spin correlation functions for the model of amorphous Gd at $T = 1$ K at different values of $J_1/|J_2|$ ratio

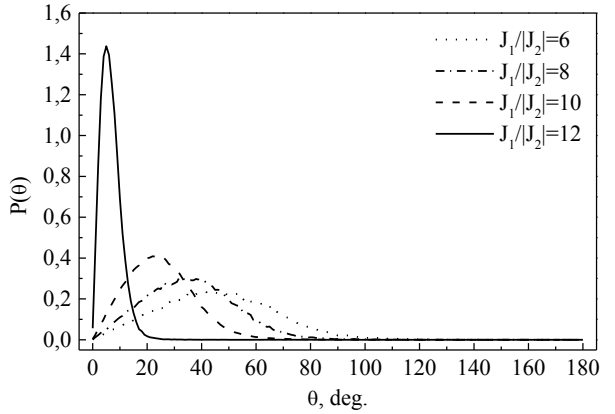

Fig. 11. Angular spin correlation functions for the model of amorphous Gd at $T = 1$ K

The $P(\theta)$ functions have one distinct maximum, its position monotonically decreases with increasing the $J_1/|J_2|$ ratio.

With increasing the temperature, the maximum on the $P(\theta)$ curve becomes lower and wider and shifts to the large angles. The position of the maximum on the angle spin correlation function linearly depends on the temperature.

References

1. K.H. Fischer, Phys. Stat. Sol. (b) **116**, 57 (1983)
2. K. Binder, A.P. Young, Rev. Mod. Phys. **58**, 801 (1986)
3. Yu.V. Barmin, S.Yu. Balalaev, A.V. Bondarev et al., Bull. Russ. Acad. Sci. Physics. **70**, 1308 (2006)
4. I.L. Bataronov, A.V. Bondarev, Yu.V. Barmin, Bull. Russ. Acad. Sci. Physics. **64**, 1329 (2000)
5. A.V. Bondarev, I.L. Bataronov, Yu.V. Barmin, Vestnik VGTU. Ser. Materialovedenie. **1.15**, 39 (2004) (*in Russian*)
6. K. Binder, Rep. Prog. Phys. **60**, 487 (1997)
7. R. Harris, M. Plischke, M.J. Zuckermann, Phys. Rev. Lett. **31**, **160** (1973)
8. A.V. Bondarev, V.V. Ozherelyev, I.L. Bataronov et al., Bull. Russ. Acad. Sci. Physics. **74**, 1474 (2010).